

Searching for extra-dimensions at CMS

This article has been downloaded from IOPscience. Please scroll down to see the full text article.

2009 J. Phys.: Conf. Ser. 171 012090

(<http://iopscience.iop.org/1742-6596/171/1/012090>)

View [the table of contents for this issue](#), or go to the [journal homepage](#) for more

Download details:

IP Address: 146.175.15.74

The article was downloaded on 15/09/2010 at 08:55

Please note that [terms and conditions apply](#).

Searching for extra-dimensions at CMS

Leonardo Benucci

Universiteit Antwerpen, Groenenborgerlaan 171, B-2020 Antwerpen, Belgium

E-mail: leonardo.benucci@cern.ch

Abstract. A possible solution to the hierarchy problem is the presence of extra space dimensions beyond the three ones which are known from our everyday experience. The phenomenological ADD model of large extra-dimensions predicts a $E_T^{miss} + \text{jet}$ signature. Randall-Sundrum-type extra-dimensions predict di-lepton and di-jet resonances. This contribution addresses an overview of experimental issues and discovery potential for these new particles at the LHC, focusing on perspectives with the CMS detector during early data taking.

The idea of using extra spatial dimensions to unify different forces started in 1914 with Nordstöm and was then elaborated by Kaluza in the framework of Theory of Gravity. More recently it was realized that extra-dimensions with a fundamental scale of order TeV^{-1} could solve the hierarchy problem between the Planck (M_{Pl}) and the electroweak scales (M_{EW}) and therefore have direct implications for next collider experiments.

In Sec. 1 some of the most relevant scenarios for experimentally accessible extra-dimensions will be sketched, underlying the signatures that could be detected at the Large Hadron Collider (LHC) experiments. As an example of this kind of searches, the determination of the Compact Muon Solenoid (CMS) detector sensitivity to the graviton production in the ADD model will be described in Sec. 2. The main message in the conclusion (Sec. 3) will be that many, very interesting insights into the extra-dimensional world will be produced even at the early stage of LHC physics runs.

1. Extra-dimension models and their signatures

1.1. Large extra-dimensions (ADD)

The phenomenological ADD model [1] aims to solve the hierarchy problem between the electroweak and Planck scales by introducing a number δ of extra space dimensions, which in the simplest scenario are compactified over a torus and all have the same radius R . The Standard Model (SM) is confined on the ordinary space-time, called *braneworld*, while gravitons can freely travel through the $4 + \delta$ -dimensional space. Since the 4-dimensional part of the metric does not depend on extra-dimensional coordinates, the Planck mass turns to be $M_{Pl}^2 \approx R^\delta M_D^{\delta+2}$, where M_D can be intended as the quantum gravity scale of the higher dimensional theory. In this way, the weakness of gravity interaction is ascribed to its “dilution” in a very large space.

A tower of Kaluza-Klein (KK) graviton modes (coupling with SM matter with gravitational strength) can be directly produced. If $2 < \delta < 6$, it turns out that $\text{fm} < R < \text{mm}$ that in the latter case corresponds to $M_D \sim \text{TeV}$.

The ADD model could be experimentally detected either via direct graviton emission in association with a photon or a jet (e.g., $q\bar{q} \rightarrow G\gamma/j$) or via virtual graviton exchange. Since gravitons are weakly coupled to ordinary matter and escape detection, in the first case the existence of the emitted graviton is deducible by a signature of missing transverse energy in a detector. The sensitivity of CMS to ADD model parameters will be outlined in the next section. Virtual graviton exchange could potentially be detected by deviations in di-lepton and di-jet cross-sections from those expected from SM processes only. CMS has studied the reach achievable in the dimuon channel [2], requiring two opposite sign muons which have an invariant mass greater than 1 TeV. The discovery reach obtained with 1 fb^{-1} ranges from 3.9 to 5.5 TeV for 6 to 3 extra-dimensions respectively.

The theoretical description above is valid for processes with typical center-of-mass energy $\sqrt{s} \ll M_D$. In the opposite limit $\sqrt{s} \gg M_D$, classical gravitation could dominate over quantum gravity effects. The Schwarzschild radius R_S for a colliding system in $4 + \delta$ dimension results to be larger than the corresponding one in ordinary space and, if the impact parameter is within R_S , gravitational collapse and black hole formation is expected. The black hole production cross section is estimated to be of order the geometric area $\sigma \approx \pi R_S^2$, that for $M_D = 1 \text{ TeV}$ corresponds to 10 pb for objects with a 6 TeV mass. The produced black hole emits thermal radiation and completely evaporates with lifetime around $10^{-26} \div 10^{-27} \text{ s}$.

The black hole should be easily detected because it emits a significant fraction of visible (i.e., non-gravitational) radiation by decaying “democratically” in all SM particles. A possible black hole decay would result in spectacular events with high multiplicity, high sphericity and high total energy. A recent ATLAS study [3] has concluded that, if the semi-classical cross section estimates are valid, black holes above a 5 TeV threshold can be discovered with a few pb^{-1} of data, while 1 fb^{-1} would allow a discovery to be made even if the production threshold is 8 TeV.

1.2. Warped extra-dimensions (RS)

In the Randall-Sundrum model [4], the hierarchy is solved by having a single highly curved (warped) extra-dimension. This fifth dimension is compactified on a circle projected into a segment and two branes are formed: the ultra-violet (UV) brane, where the graviton function is peaked, and the infra-red (IR) brane, that appears to be “red-shifted” from the former following the relation: $m_{IR} \sim m_{UV} \exp(-\pi kR)$. With $m_{UV} \sim M_{Pl}$, m_{IR} can be reduced to the TeV scale if the curvature of this extra-dimension is such that $kR = 11 \div 12$.

If the coupling to the IR brane is of the order of TeV^{-1} , a resonant and on-shell production of the KK excitations gravitons is possible at LHC, leading to characteristic peaks in the di-lepton, di-photon or di-jet invariant mass spectra. Recent studies from CMS have addressed both the $G \rightarrow ee$ [5] and the $G \rightarrow \mu\mu$ [6] channels. The result for the muon channel is shown in Fig. 1 and indicates that an RS graviton with mass 1 TeV can be discovered by CMS after $10(5000) \text{ pb}^{-1}$ if the coupling parameter is $k/M_{Pl} = 0.1(0.01)$.

1.3. Universal extra-dimensions (UED)

Not only gravity, but also SM fields could live in an experimentally accessible higher-dimensional space. The case in which all SM particles uniformly propagate in the bulk of an extra-dimensional space is referred to as Universal Extra Dimensions [8]. The absence of a reference brane that breaks translation invariance in the extra-dimensional direction implies extra-dimensional momentum conservation, corresponding to the invariance of a discrete symmetry called KK-parity. Since the KK-parity of the n^{th} KK mode of each particle is $(-1)^n$, in UED the first KK excitations can only be pair-produced and their virtual effect comes only from loop corrections. Therefore the ability to constrain parameter space is diminished and limits on R^{-1} are less

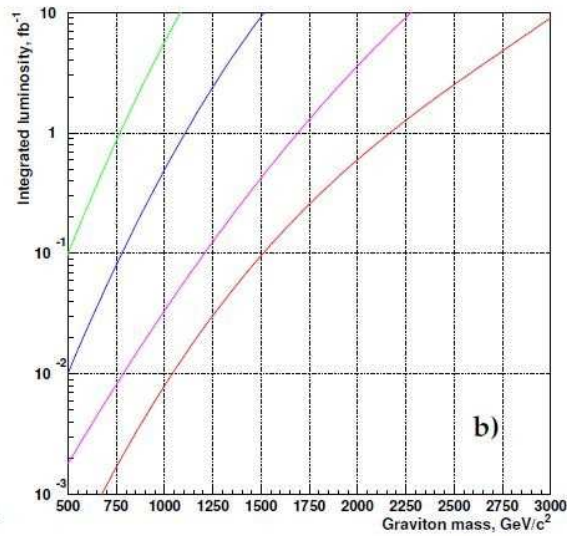


Figure 1. Integrated luminosity needed to reach 5σ significance for a RS1 gravitons with the coupling constant of (from top to bottom) 0.01, 0.02, 0.05, and 0.1 [6].

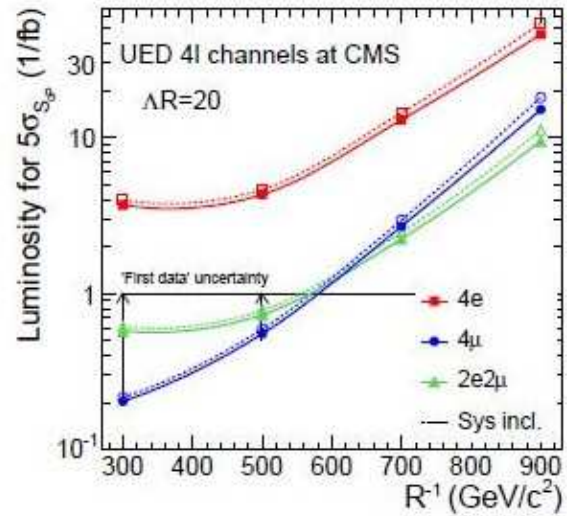


Figure 2. Discovery potential of UED signals in four lepton final state. The dotted lines show the influence of experimental uncertainties and the background cross-section uncertainty [7].

bound (between 300 and 500 GeV). The lightest KK state has to be stable, thus one interesting consequence of the model is the possibility of the lightest KK to be a dark matter candidate.

CMS discovery potential for UED has been inquired for four values of the compactification radius, looking at decays in 4μ , $4e$ and $2\mu 2e$ final state [7]. The discovery potential at 5σ level is reported in Fig. 2 as the result of interpolating the points at different curvature. It indicates that a leptonic UED signal can be discovered with the first hundreds of integrated pb^{-1} , if the curvature of the bulk is below $500 \div 600 \text{ GeV}$.

2. Mono-Jet Final States from ADD Extra Dimensions in CMS

The following section is an outline of procedures that will be used to search for evidence of ADD extra-dimensions in the missing transverse energy plus a single jet ($E_T^{\text{miss}} + 1 \text{ jet}$) channel, using the CMS detector [9], for an integrated luminosity of up to 100 pb^{-1} and 7 TeV proton beams.

The new physics signal addressed in this study has a simple signature:

- A high-transverse momentum ($> 300 \div 400 \text{ GeV}$) jet in the central region ($|\eta| < 1.7$), possibly accompanied by less energetic jets from initial or final state gluon radiation. No other energetic jets are produced, neither central nor in the very forward direction, creating a typical ‘mono-jet’ signature;
- a large E_T^{miss} (same order of magnitude of jet p_T) emerging almost back-to-back to the leading jet in the transverse plane.

Several Standard Model processes may mimic such a topology. This study addresses the most relevant ones: Z +jets with the Z decaying into two neutrinos (‘irreducible’ background); W +jets followed by a leptonic W decay (faking the signal when the lepton is not reconstructed); QCD di-jets (when one or more jets are mismeasured and/or a significant amount of E_T^{miss} is produced by hadron decays); top quark production (both $t\bar{t}$ and single-top, contributing when missing energy and energetic jets point in opposite directions).

This study is focused on the production of a graviton balanced by a energetic hadronic jet via the $q\bar{q} \rightarrow gG$, $qg \rightarrow qG$, and $gg \rightarrow gG$ processes. The ADD model signal has been produced thanks to the SHERPA generator [10] version 1.0.11. In order to explore the sensitivity in a wide energy spectrum, 18 different samples with M_D ranging from 2 to 7 TeV and $\delta = 2, 3, 4$ have been produced. Since the ADD cross sections are usually computed in an effective theory approach [11], the cut prescription $\sqrt{\hat{s}} < M_D$ has been introduced in the generation step. A p_T cut-off $\hat{p}_T > 200$ GeV on the parton¹ recoiling against the graviton was also introduced. With these production parameters, signal cross sections (LO) are evaluated by SHERPA for the 18 samples and found to range from 49.2 pb (for $M_D = 2$ TeV, $\delta = 2$) to 0.11 pb (for $M_D = 6$ TeV, $\delta = 4$).

The set of background processes has been generated with a sample size corresponding to an integrated luminosity of 100 pb^{-1} or more, with the exception of low \hat{p}_T QCD samples. All the boson+jets and $t\bar{t}$ samples have been produced with ALPGEN 2.12 [12] with $0 < \hat{p}_T < 3200$ GeV for W/Z +jets, while large multijet QCD background was generated by PYTHIA 6.409 [13]. The standard software framework adopted by the CMS collaboration (CMSSW) was exploited in the whole simulation and reconstruction chain. Data samples have been reconstructed with calibration and alignment constants based on the detector calibration stage expected for 100 pb^{-1} of data.

2.1. Signal and background analysis

In all the analyses reported here, the trigger is based on the sum H_T and the module of the vectorial sum MH_T of transverse momenta of all jets above p_T^0 . The trigger thresholds are $H_T > 200$ GeV and $p_T^0 = 10$ GeV at first level trigger (L1), followed by $H_T > 250$ GeV, $MH_T > 100$ GeV and $p_T^0 = 20$ GeV at High Level Trigger (HLT).

The set of cuts used are detailed in Ref. [14]. A cut $E_T^{miss} > 400$ GeV is imposed early in the selection. To clean the events from isolated lepton contamination and electrons and photons misidentified as jets, the fraction of jet energy collected by the electromagnetic calorimeter over the total energy is required to be lower than 0.9 and isolated tracks (having less than 10% of p_T in a $0.02 < \Delta R < 0.35$ cone) are removed. The leading jet is required to have $p_T(\text{jet } 1) > 350$ GeV and $|\eta(\text{jet } 1)| < 1.7$. A veto against events with more than two jets and a number of angular cuts $\Delta\phi(\text{jet } 1, E_T^{miss}) > 2.8$ and $\Delta\phi(\text{jet } 2, E_T^{miss}) > 0.5$ complete the selection.

Missing energy distributions for signal and background are shown in Fig. 3, after the complete set of selections has been applied. A clear excess of events appears on top of $Z(\nu\nu)$ +jets with a large E_T^{miss} tail.

The effect of each group of cuts is reported in Tab. 1 for all the Standard Model processes and in Tab. 2 for some benchmark signals. The absolute expected number of events is shown for 100 pb^{-1} of data. Table 2 confirms that both the kinematic and geometric features of the reconstructed ADD signal are uniform for M_D from 2 to 6 TeV and δ from 2 to 4, thus the selection efficiencies are consistent within the statistical uncertainties. The numbers of events are found to scale with the cross section, which decreases as $1/M_D^{\delta+2}$.

2.2. Data-driven background estimation

In the following, procedures are proposed to evaluate the irreducible background of $Z(\nu\nu)$ +jets (here referred also as “invisible Z” background) and $W(e/\mu/\tau\nu)$ +jets. The aim is to derive the background contributions with as little Monte Carlo dependence as possible, in order to minimize hard-to-control simulation uncertainties.

¹ Hereafter, \hat{p}_T is intended as the transverse momentum of the outgoing parton in jet production (gluon or quark).

Table 1. Number of selected events for each group of cuts in the relevant background samples, normalized to 100 pb^{-1} .

	$t\bar{t}$	$Z(\nu\nu)+\text{jets}$	QCD	$W(e\nu)+\text{jets}$	$W(\mu\nu)+\text{jets}$	$W(\tau\nu)+\text{jets}$
Trigger	3860	1280	$4.92 \cdot 10^5$	1199	1617	1488
$E_T^{miss} > 400 \text{ GeV}$	36.6	54.8	17.9	19.5	63.7	36.3
$JEMF < 0.9$	32.0	52.4	17.2	8.8	60.6	32.0
$TIV < 0.1$	12.2	46.3	14.2	4.3	5.9	13.0
$p_T(\text{jet } 1) > 350 \text{ GeV}$, $ \eta(\text{jet } 1) < 1.7$	9.8	36.6	11.8	3.3	4.5	9.9
Number of jets < 3	2.2	28.9	4.6	2.3	2.8	6.9
$\Delta\phi(\text{jet } 1, E_T^{miss}) > 2.8$, $\Delta\phi(\text{jet } 2, E_T^{miss}) > 0.5$	0.5	25.7	< 0.6	2.0	2.0	5.5

Table 2. Number of selected events for each group of cuts in four signal subsamples, normalized to 100 pb^{-1} . Uncertainties on efficiencies are statistical only.

	$\delta = 2$		$\delta = 4$	
	$M_D = 2 \text{ TeV}$	$M_D = 6 \text{ TeV}$	$M_D = 2 \text{ TeV}$	$M_D = 6 \text{ TeV}$
Trigger	3060	54.4	1190	7.98
$E_T^{miss} > 400 \text{ GeV}$	691	12.1	244.7	3.05
$JEMF < 0.9$	658.6	11.6	231.8	2.9
$TIV < 0.1$	539.2	9.5	185.2	2.2
$p_T(\text{jet } 1) > 350 \text{ GeV}$, $ \eta(\text{jet } 1) < 1.7$	343.1	6.5	117.1	1.6
Number of jets < 3	286.8	5.4	98.3	1.2
$\Delta\phi(\text{jet } 1, E_T^{miss}) > 2.8$, $\Delta\phi(\text{jet } 2, E_T^{miss}) > 0.5$	261.5	4.9	90.1	1.1
Total Efficiency (%)	8.1 ± 0.5	8.5 ± 3.8	7.1 ± 0.7	13.2 ± 13.2

In Ref. [15] it has been shown how the Z invisible background can be deduced from samples of events containing a high- p_T $W(\rightarrow l\nu)$ boson. The E_T^{miss} spectrum is obtained by removing the identified lepton and correcting for residual differences between these events and invisible Z events.

The selection defining the control region has been kept as close as possible to that of the $E_T^{miss} + 1 \text{ jet}$ signal, except that one muon with $p_T > 20 \text{ GeV}$ is required. The muon is used to trigger the event and must be isolated with $\mu_{Iso} < 1 \text{ GeV}$, where $\mu_{Iso} = \sum_{trk}^{\Delta R} p_T(\text{trk})$ and $\Delta R = 0.3$. Since the requirement of an isolated muon reduces the effect of the lepton cleaning algorithm, important contaminations from $t\bar{t}$ and $W(\tau\nu)$ affect the control region and have to be accounted for.

From simulations, the shapes of the missing energy distributions have been proven to be quite similar for the $W(\tau\nu)+\text{jet}$ and $W(\mu\nu)+\text{jet}$ processes, so the ratio determined from Monte Carlo could be used to retrieve the number $W(\tau\nu)+\text{jet}$ from $W(\mu\nu)+\text{jet}$, with little systematic uncertainty. As a cross-check of this method, it has been observed that all $W(\tau\nu)$ events entering the region have a muon from τ decay. Therefore, the composition of the control region can be assumed to be $N^{Contr} = [1 + Br(\tau \rightarrow \mu\nu\nu)] N(W(\mu\nu) + \text{jets})^{Contr} + N(t\bar{t})^{Contr}$.

The remaining fraction of $t\bar{t}$ is considered as a contamination of the control region and included as a systematic bias. With $Br(\tau \rightarrow \mu\nu\nu) = 0.1736 \pm 0.0005$, the method produces the number of events in the control region $N(W(\mu\nu) + \text{jets})^{Contr} = 19.9 \pm 4.5$ (stat) $_{-0.0}^{+1.6}$ (syst), which is consistent with the Monte Carlo result. Subtracting this value from the control region leads to a $N(W(\tau\nu) + \text{jets})^{Contr} = 3.45 \pm 0.77$ (stat) $_{-0.0}^{+0.27}$ (syst), to be compared with the expected 3.32 events.

To reproduce the number of $Z(\nu\nu) + \text{jets}$ invisible background, the number of selected $W(\mu\nu) + \text{jets}$ has to be rescaled accounting for the ratio between $Z(\nu\nu) + 1 \text{ jet}$ and $W(\mu\nu) + 1 \text{ jet}$ production cross sections, the muon reconstruction and isolation efficiency and the trigger efficiency for the single-muon trigger stream. These efficiencies can be estimated with a standard ‘Tag and Probe’ method with small statistical and systematic uncertainties [15, 16].

Applying all the correction factors with their uncertainty, the number of invisible Z events in the signal region is found to be $N(Z(\nu\nu) + \text{jets})^{Sig} = 21.9 \pm 4.9$ (stat) $_{-1.4}^{+2.1}$ (syst). The two shapes are consistent and confirm that the $W(\mu\nu) + \text{jet}$ process can be used to estimate the $Z(\nu\nu) + \text{jet}$ background.

As quoted in Tab. 1, the $W + \text{jet}$ background followed by a $W \rightarrow \tau\nu$ decay can contribute up to $\sim 16\%$ of the total background. These events can be estimated in a data-driven way by using again the control region addressed above. Beside the irreducible contribution, that region is composed of $W + \text{jets}$ decaying to $\mu\nu$ (79%) or $\tau\nu$ (13%) final states and $t\bar{t}$ (8%). The latter component has been subtracted from the background and considered as a systematic contamination. Since it is expected to be measured with a 8% precision with 100 pb^{-1} [17], the number of top events can be normalized without relying on theoretical expectations.

The contribution of $W(\tau\nu) + \text{jets}$ in the signal region can be derived in a similar way and results in $N(W(\tau\nu) + \text{jets})^{Sign} = 4.89 \pm 1.09$ (stat) $_{-0.39}^{+0.46}$ (syst). When the procedure is applied to the other W channels, it produces $N(W(\mu\nu) + \text{jets})^{Sign} = 1.76 \pm 0.39$ (stat) $_{-0.14}^{+0.17}$ (syst) and $N(W(e\nu) + \text{jets})^{Sign} = 1.75 \pm 0.39$ (stat) $_{-0.13}^{+0.16}$ (syst). All these values are consistent with the direct Monte Carlo estimates reported in Tab. 1.

2.3. Impact of systematic effects

An overview of the effects induced by theoretical and instrumental uncertainties is summarized in Table 3.

To estimate the cross-section sensitivity to theoretical errors, the renormalization and factorization scale has been varied from $Q/2$ to $2Q$ (where $Q = \sqrt{\hat{s}}$), and uncertainties based on the CTEQ6M [18] error PDF’s have been derived.

The uncertainty on the jet energy scale has been reproduced by shifting the jet 4-vector with a common $(1 \pm \alpha)$ factor and repeating the analysis. For this early LHC stage, $\alpha = 10\%$ can be conservatively assumed irrespectively of the jet energy.

Missing transverse energy has been obtained from calorimeter towers, so the uncertainty on energy deposits can have an additional effect on the number of events passing the 400 GeV cut on E_T^{miss} . The effect has been simulated applying a $\pm\sigma(E_T^{miss})$ shift to the uncorrected missing transverse energy, where $\pm\sigma(E_T^{miss})$ is the E_T^{miss} resolution determined from the calorimeter measurement and can be found in Ref. [19]. Systematic uncertainties due to E_T^{miss} resolution and jet energy resolution were found to be negligible: after a gaussian smearing of energy (by 10%) and ϕ angle (by 0.1 rad), the maximum effect is 3% on signal efficiency while the S/B is almost unaffected. The uncertainty on the instantaneous luminosity was taken to be $\pm 10\%$. The jet energy and the E_T^{miss} correlation has not been checked in detail, but a preliminary study shows that the two quantities are completely correlated. Therefore, the effects from scale variation have been summed linearly.

Table 3. Overview of the effect from systematic uncertainties considered in the analysis. Superscripts/subscripts in the second column correspond to $+/-$ variation imposed on parameters, respectively. Total theoretical uncertainty includes PDF and hard process scale (summed quadratically) while total instrumental uncertainty sums linearly the contributions of E_T^{miss} and jet energy scale.

Source	Effect on number of signal events (%)
Hard process scale	+11 -13
PDF	+8.7 -6.7
Jet energy scale (10%)	-0.8 -4.0
E_T^{miss}	+17.5 -15.9
Total theoretical uncertainty on signal	+14.0 -14.6
Total instrumental uncertainty on signal	+16.7 -19.9
Luminosity with 100 pb^{-1}	10.0

2.4. Discovery potential and exclusion limits

A first estimate for the mono-jet discovery reach can be obtained by considering all the relevant background sources, the ADD signal efficiency, and the impact of systematic effects. Combining the results from the previous section, the total background can be quoted as:

$$N_B = 30.7 \pm 6.8 \text{ (stat)}_{-1.5}^{+2.7} \text{ (syst) events}$$

expected for 100 pb^{-1} of integrated luminosity.

The significance estimator S_{PL} (Profile Likelihood) from Ref. [20] (and references therein) is chosen. It can be computed from a likelihood ratio, where the likelihood function is a Poisson distribution for the total number of observed event ($N_S + N_B$). Using S_{PL} and the results for different values of M_D , δ , a discovery sensitivity plot is derived as a function of the M_D and displayed in Fig. 4. Systematic errors on the signal are incorporated in the N_S estimate. It has been verified that a decrease of the luminosity uncertainty down to 7% does not change significantly the results.

Evidence for an $E_T^{miss} + 1$ jet signal can be obtained for values of the fundamental scale M_D lower than 3.58 (2.62) TeV for $\delta = 2(4)$, while 95% C.L. exclusion limits are expected to be 4.12 (3.12) TeV for $\delta = 2(4)$. The current best lower limits on M_D at 95% confidence level (C.L.) are 1.600 (1.040) TeV for $\delta = 2(4)$, from the LEP [21] and Tevatron [22, 23] experiments.

3. Conclusions

In this conference report we outlined how the hierarchy problem can be solved with different extra-dimension model, which imply new phenomena that could be visible at the LHC scale. Kaluza-Klein modes foreseen by the Randall-Sundrum framework, for instance, can be probed in a wide energy spectrum and very interesting possibilities are opened for UED and black hole production, even in a quite early LHC stage. If extra-dimensions in the ADD model are large enough, we showed that current limits on M_D can be improved by a factor 3 with CMS detector, even with low integrated luminosity and sub-optimal performance. Techniques to evaluate background from future data-samples are in place and results are robust against several background sources.

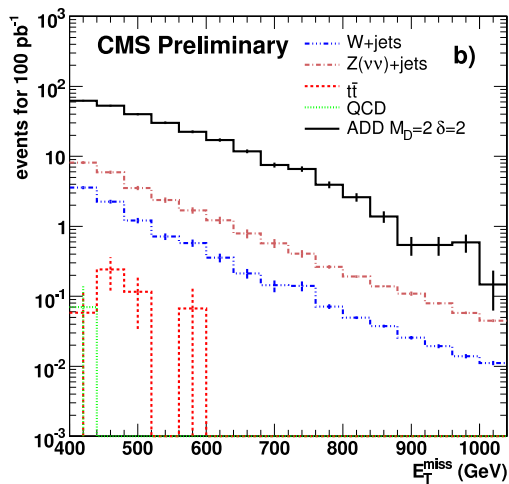


Figure 3. Missing transverse energy distribution after all selections are applied. Histograms are overlaid, not stacked.

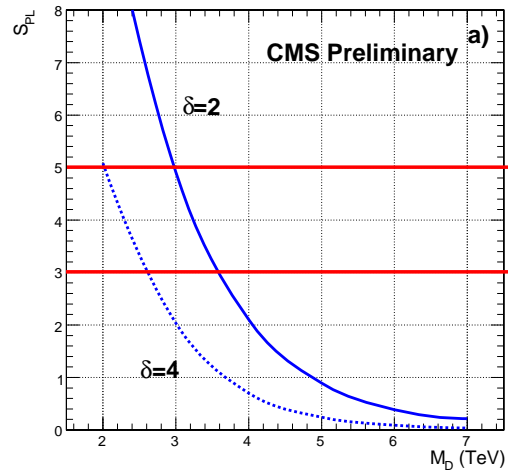


Figure 4. Discovery potential of the analysis as a function of M_D and δ . The significance estimator S_{PL} is defined in the text and the assumed integrated luminosity is 100 pb^{-1} .

References

- [1] Arkani-Hamed N, Dimopoulos S and Dvali G R 1998 *Phys. Lett.* **B429** 263 (Preprint hep-ph/9803315)
- [2] CMS Collaboration 2006 *J. Phys. G: Nucl. Part. Phys.* **34** 995
- [3] Aad G Tech. rep.
- [4] Randall L and Sundrum R 1999 *Phys. Rev. Lett.* **83** 3370
- [5] CMS Collaboration 2008 *CMS-PAS-EXO-08-001*
- [6] CMS Collaboration 2008 *CMS-PAS-SBM-07-002*
- [7] Kazana M 2008 *CMS-CR-2006/062*
- [8] Appelquist T, Cheng H C and Dobrescu B A 2001 *Phys. Rev. D* **64** 035002
- [9] CMS Collaboration 2007 *Journal of Physics G: Nuclear and Particle Physics* **34** 995 URL <http://stacks.iop.org/0954-3899/34/995>
- [10] Gleisberg T, Hoeche S, Krauss F, Schaelicke A, Schumann S and Winter J 2004 *JHEP* **0402** 056 (Preprint hep-ph/0311263)
- [11] Giudice G F, Rattazzi R and Wells J D 1999 *Nucl. Phys.* **B544** 3 (Preprint hep-ph/9811291)
- [12] Mangano M L, Moretti M, Piccinini F, Pittau R and Polosa A D 2003 *JHEP* **0307** 001 (Preprint hep-ph/0206293)
- [13] Sjostrand T *et al.* 2001 *Computer Physics Communications* **135** 238 (Preprint hep-ph/0010017)
- [14] CMS Collaboration 2008 *CMS-PAS-EXO-08-011*
- [15] CMS Collaboration 2008 *CMS-PAS-SUS-08-002*
- [16] CMS Collaboration 2007 *CMS-PAS-EWK-07-002*
- [17] CMS Collaboration 2008 *CMS-PAS-TOP-08-002*
- [18] Pumplin J *et al.* 2002 *JHEP* **07** 012 (Preprint hep-ph/0201195)
- [19] CMS Collaboration 2007 *CMS-PAS-JME-07-001*
- [20] Cousins R D, Linnemann J T and Tucker J 2008 *NIM* **A595** 480 (Preprint physics/0702156v3)
- [21] Krutelyov V 2008 (Preprint 0807.0645)
- [22] CDF Collaboration 2008 (Preprint 0807.3132)
- [23] D0 Collaboration 2008 *Physical Review Letters* **101**